



Installation and interference drag decomposition via RANS far-field methods



Benoit Malouin*, Jean-Yves Trépanier, Éric Laurendeau

Polytechnique Montréal, Dept. of Mechanical Engineering, 2900 Boul. Edouard-Montpetit, Montréal, Québec H3T 1J4, Canada

ARTICLE INFO

Article history:

Received 16 July 2015

Received in revised form 17 April 2016

Accepted 19 April 2016

Available online 22 April 2016

Keywords:

CFD

Drag

Thrust

Far-field

Power-on

Bookkeeping

ABSTRACT

Computation of the engine installation drag is important to both airframers and engine manufacturers who wish to assess performance of their respective system. This force comprises the interference drag that results from the interaction between the wing and the engine's nacelle. Its evaluation is cumbersome because of the coupled nature of this phenomenon. It is thus proposed to decompose the installation drag in terms of interference and nacelle drags that, using the far-field method, can be further discretized in terms of viscous, wave, induced, spurious and pre-entry forces. By using simulations on the isolated nacelle, the wing-body and the wing-body-pylon-nacelle configurations, it is thus possible to compute and decompose both the interference and installation drags. Simulations are performed with ANSYS Fluent 14.5 on the DLR-F6 equipped with CFM56 nacelles in power-on conditions. A far-field method to compute and decompose the installation and interference drags is thus introduced for the first time. Results have shown that the installation and interference drags in powered conditions account for more than 25% and 5% of the total configuration drag, respectively. It is also shown that the viscous drag and the pre-entry thrust are the two main contributors to the installation drag, each accounting for about 40%.

© 2016 Elsevier Masson SAS. All rights reserved.

1. Introduction

Global trends in fuel prices have lead airframers toward the use of very-high and ultra-high-bypass-ratios turbofan engines, which are more powerful and efficient than older generations engines [1]. However, the gain in power efficiency is partially overshadowed by the increase in installation drag in part due to higher wetted area. The installation drag is traditionally computed by subtracting the wing-body drag D^{WB} and the nacelle internal drag D^{scrub} from the wing-body-pylon-nacelle drag D^{WBPN} . The installation drag is composed of the nacelle and the interference drags. The latter is difficult to evaluate since it represents a coupled phenomenon involving the wing and the nacelle. The objective of this paper is to propose a method to estimate the installation and interference drags using the far-field approach.

The development of the far-field drag decomposition method made possible the identification of the main cause of drag creation for a given configuration in terms of physical phenomena producing drag such as the boundary layer and the shock wave phenomena [2–5]. Later, Tognaccini [6] and, Van der Vooren and

Destarac [7] applied this method to powered configurations. Recently, Malouin et al. [8] proposed a new method to compute the pre-entry thrust and the standard net thrust based solely on the far-field theory yielding a more accurate method to study powered configurations. With all these tools available, it is now possible to decompose the installation drag. In this paper, we propose to decompose this force into two major components: the nacelle drag and the interference drag. For each, the far-field method, based on entropy generation, allows separation of each component in terms of the physical phenomena accountable for drag production.

In this paper, the chosen configuration is the DLR-F6 since it is public and is supplemented with experimental data in power-off conditions [9]. The lack of either numerical or experimental data in power-on conditions makes it difficult to validate the results. To overcome this issue, we propose to proceed via a step by step procedure. First, the DLR-F6 with through-flow nacelle (TFN) is simulated and results are validated with the available experimental data. Then, the TFN is replaced by a turbine powered simulator (TPS) with power-on boundary conditions used to reproduce the TFN flow. To verify the implementation of the TPS boundary conditions, the configuration drags are compared. Since the flow is the same, the configuration drags of both the TFN and TPS cases should be equal. In fact, there is a small discrepancy which is explained by the inclusion of the boundary conditions. Nevertheless,

* Corresponding author.

E-mail address: benoit.malouin@gmail.com (B. Malouin).

Nomenclature

α	Angle of attack..... °	S_{ref}	Reference area..... m ²
ΔH	Enthalpy variation from free stream..... J/kg	T	Thrust..... N
Δs	Entropy variation from free stream..... J/K	T_B	Basic thrust..... N
$\Delta \bar{u}$	Axial velocity defect..... m/s	T_{int}	Intrinsic thrust..... N
γ	Ratio of specific heats	T_N	Standard net thrust..... N
μ	Viscosity..... N·s/m ²	T_{pre}	Pre-entry thrust..... N
∇p	Pressure gradient..... kPa/m	$\vec{\tau}_x = [\tau_{xx}, \tau_{xy}, \tau_{xz}]$	Viscous stresses vector..... N/m ²
ρ	Density..... kg/m ³	\vec{f}, \vec{f}_x	Momentum vectors
D_A	Nacelle external drag..... N	f_i	Momentum vector associated with reversible processes
D_c	Configuration drag..... N	\vec{f}_{vw}	Momentum vector associated with irreversible processes
D_f	Friction drag..... N	\vec{i}	X-direction unit vector
D_{irr}	Irreversible drag..... N	$\vec{n} = [n_x, n_y, n_z]$	Normal vector
D_i	Induced drag..... N	$\vec{V} = [u, v, w]$	Velocity vector..... m/s
D_{NF}	Near-field drag..... N	p	Static pressure..... kPa
D_p	Pressure drag..... N	S_c	Surface of the configuration
D_{scrub}	Scrubbing drag..... N	a	Speed of sound..... m/s
D_{sp}	Spurious drag..... N	c	Chord..... m
D_{tf}	Additive through-flow drag..... N	F	Net propulsive force..... N
D_v	Viscous drag..... N	MFR	Mass flow ratio
D_w	Wave drag..... N	R	Gas constant..... J/(kg·K)
F_{FF}	Far-field net propulsive force..... N		
F_{NF}	Near-field net propulsive force..... N		
M_∞	Free stream Mach number		

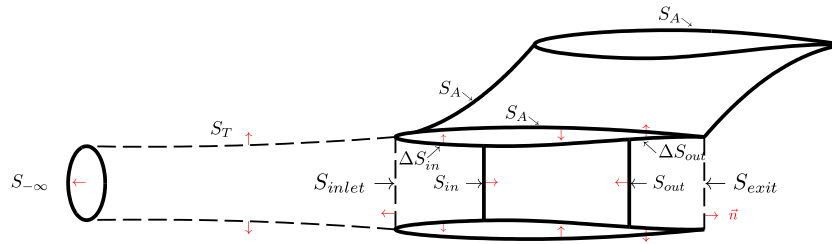


Fig. 1. Isolated nacelle geometry and surfaces.

results are in good agreement and this discrepancy is further detailed. The next step is to compute and decompose the installation drag on the DLR-F6 TPS case, but still without thrust. The presence of those boundary conditions leads to the use of the configuration drag instead of the typical near-field net propulsive force which could be negative because of thrust generation. The advantage of this modification is that the pre-entry thrust of the nacelle can be computed and included in the installation drag. Since there is no available data for validation, the installation drag is validated based on the near-field/far-field balance which is in good agreement. Finally, thrust is added to the configuration by increasing the total pressure and total temperature ratios. Again, the installation drags are in good agreement.

The next section presents an overview of the far-field theory to compute drag and thrust and thrust/drag bookkeeping in CFD. It is followed by the development of the proposed approach to separate the installation drag in terms of nacelle and interference drags.

2. Theory

The difference between the configuration drag D_c and the thrust T is the net propulsive force $F = D_c - T$, which is constant at given flow conditions for a given configuration. However, many definitions for the thrust are available and, regarding the user's choice, the thrust and the drag can vary. In the following section, forces on a motorized aircraft are described. It is followed by a summary of the far-field method used to compute these forces.

Then, new approaches to compute the standard net thrust and the pre-entry thrust are proposed.

2.1. Forces on configuration

Consider the isolated nacelle in power-on conditions depicted in Fig. 1. Note that the small red arrows represent the normal vectors. The forces applied to this configuration are:

- Pre-entry thrust
- Standard net thrust
- Basic thrust
- Scrubbing drag
- Aircraft drag

The pre-entry thrust T_{pre} , also known as additive drag, corresponds to the difference in stream forces between the nacelle entry and the streamtube capture area located infinitely far upstream (S_∞) [10]. This force appears when the mass flow ratio is different than unity. The mass flow ratio MFR can be computed as follows:

$$MFR = \frac{S_\infty}{S_{inlet}} \tag{1}$$

where S_{inlet} is determined by the nacelle's most forward points plane. In this paper, the hypothesis is made that the shear stress is negligible on the streamtube surface S_T because it is far from a

Download English Version:

<https://daneshyari.com/en/article/8058561>

Download Persian Version:

<https://daneshyari.com/article/8058561>

[Daneshyari.com](https://daneshyari.com)